

Chapter 6: Chronology

6.1	<i>²¹⁰Pb Sources and Pathways</i>	48
6.2	<i>Principles of ²¹⁰Pb Dating</i>	48
6.3	<i>Sediment Core Radionuclide Chronology</i>	51
6.5	<i>Sediment Core Trace Metal Chronology</i>	57

6.0 Chronology

The results from Chapter 5 suggest that the Blelham Tarn sediment cores contain good records of atmospherically delivered contaminants to the lake. Detailed interpretation and analysis of these records does however require accurate dating. The most widely used method for dating sediments on a time-scale of 100-150 years is by the natural radionuclide ^{210}Pb . Since ^{210}Pb dating is not always unambiguous, the method is supported by dates determined from stratigraphic records of the artificial radionuclides ^{137}Cs and ^{241}Am . Since ^{210}Pb is also used as a tracer in studying transport processes through the lake and its catchment, the first part of this chapter gives a brief account of the origins of ^{210}Pb fallout and its application to dating. The second part of this chapter deals with the calculation of anthropogenic atmospheric fluxes, using the sediment chronology that has just been established.

6.1 ^{210}Pb Sources and Pathways

Fallout ^{210}Pb derives from the radioactive decay (Fig. 6.1) of gaseous radon-222 (^{222}Rn) ($t_{1/2} = 3.8$ d) introduced into the atmosphere by diffusion from soils (Jaworowski *et al.*, 1972) and is normally assumed to have a constant flux at any given site (when averaged over a period of a year or more). The amount of fallout may however vary from place to place by an order of magnitude, depending on factors such as rainfall and geographical location.

Overall levels of fallout in central Europe are however significantly higher than in Great Britain, presumably due to a build of ^{222}Rn concentrations in the atmosphere as the prevailing winds transport air masses over the earth's surface. Appleby (1998) has shown that there is a consistent west to east increase in ^{210}Pb fallout within the major continents, superimposed on a baseline ^{210}Pb flux of *c.* 30-40 $\text{Bq m}^{-2} \text{y}^{-1}$ per metre of rain at sites remote from major landmasses.

Direct and indirect measurements of ^{210}Pb and ^{137}Cs deposition have been made at a number of sites in the UK during this century. The average annual flux of ^{210}Pb in the UK based on these results is 77 ± 14 $\text{Bq m}^{-2} \text{y}^{-1}$ per metre of rainfall (Smith *et al.*, 1997).

6.2 Principles of ^{210}Pb Dating

The basic methodology of ^{210}Pb dating was first outlined by Goldberg (1963) in studies of the accumulation rates of ice sheets. The adaption of these techniques by Krishnaswami *et al.* (1971) to the dating of lake sediments has revolutionised the use of lake sediment records in studies of recent environmental change. To date a ^{210}Pb chronology has become one of the standard tools of palaeolimnology, providing reliable sediment dates and accumulation rates in a large number of studies from a wide range of environments.

^{210}Pb occurs naturally in most soils as one of the radionuclides in the uranium-238 (^{238}U) decay series. Disequilibrium between ^{210}Pb and its parent isotope in the series, ^{226}Ra , arises through diffusion of the intermediate gaseous isotope ^{222}Rn . A fraction of the ^{222}Rn is introduced into the atmosphere by

diffusion from soils and rocks and decays to ^{210}Pb . This is removed from the atmosphere by precipitation or dry deposition, falling onto the land surface or into lakes and oceans. ^{210}Pb falling directly into lakes is scavenged from the water column and deposited on the bed of the lake with the sediments. Excess ^{210}Pb in sediments over that in equilibrium with the in-situ ^{226}Ra decays and can be used to date the sediment provided reliable estimates can be made of the initial ^{210}Pb activity in each sediment layer at the time of its formation.

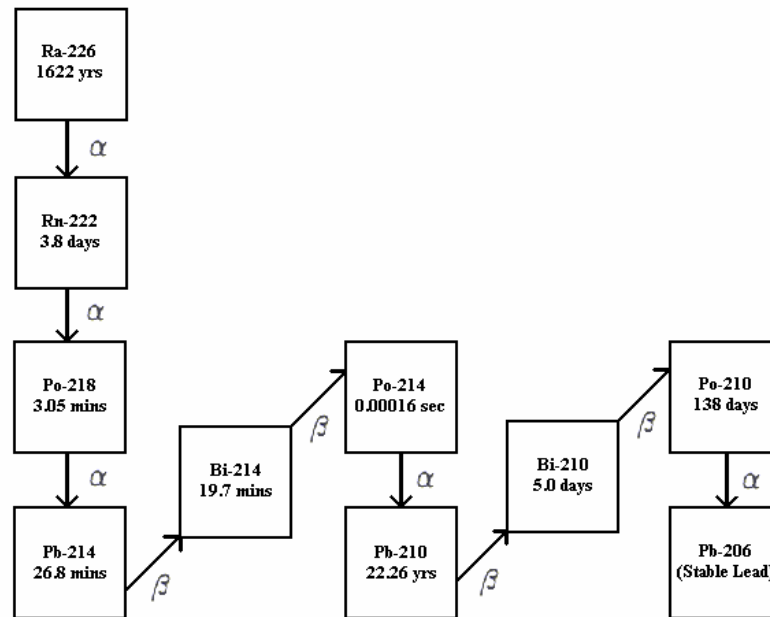


Fig. 6.1: The Uranium decay series.

The first decade of ^{210}Pb dating was characterised by the development of two simple models. The assumptions used in the original paper by Krishnaswami *et al.* (1971), were:

- the rate of deposition of unsupported ^{210}Pb from the atmosphere is constant,
- ^{210}Pb in fresh waters is quickly removed from solution onto particulate matter so that unsupported ^{210}Pb activity in sediments is essentially that due to overhead fallout from the atmosphere, and
- the initial unsupported ^{210}Pb activity in sediments laid down on the bed of the lake is not redistributed by post-depositional processes and it decays exponentially with time in accordance with the radioactive decay law.

Early use of this technique focussed on sites where sedimentation rates were more or less constant (Koide *et al.*, 1973; Robbins and Edgington, 1975). Where this is the case, the assumptions of

Krishnaswami *et al.* (1971) dictate that unsupported ^{210}Pb activity should decline exponentially with depth at a rate that is inversely proportional to the sedimentation rate.

In what is now called the Constant Initial Concentration model (CIC) the age of sediments (t) will be related to the depth (m) by

$$t = \frac{m}{r} \quad \text{eqn. 6.1}$$

where

m denotes the depth in the core (g cm^{-2}), and

r denotes the sedimentation rate ($\text{g cm}^{-2} \text{y}^{-1}$).

The unsupported ^{210}Pb activity will thus vary with depth in accordance with the formula

$$C(m) = C(0)e^{-\lambda m / r} \quad \text{eqn. 6.2}$$

where

λ is the ^{210}Pb radioactive decay constant (yr^{-1}), and

$C(0)$ is the unsupported activity at the surface of the core.

When plotted on a logarithmic scale the resulting ^{210}Pb activity versus depth profile will appear linear and the mean sedimentation rate, r , can then be determined using a least squares fit procedures. Krishnaswami *et al.* (1971) do however point out that their basic equations are not restricted to uniform sedimentation rates.

In view of the dramatic environmental changes that have occurred over the past 150 years, rates of erosion and sediment accumulation may be expected to have varied significantly during this period. Where this has occurred, unsupported ^{210}Pb activity will vary with depth in a more complicated way and ^{210}Pb profiles (plotted logarithmically) will be non-linear. Studies of sites with a variable sedimentation rate were carried out by Appleby and Oldfield (1978) and Robbins (1978). The methodology for calculating dates developed in these papers but within the assumptions set out by Krishnaswami *et al.* (1971) has become known as the Constant Rate of ^{210}Pb Supply (CRS) or Constant ^{210}Pb Flux (CF) model.

Briefly summarised from Appleby (1984), if

$$A(m) = \int_m^\infty C(m) dm \quad \text{eqn. 6.3}$$

is the unsupported ^{210}Pb inventory beneath sediments of depth m (g cm^{-2}) and age t , then it is shown that the age t of sediments of depth m satisfies the equation

$$A(m) = A(0) e^{-\lambda t}, \quad \text{eqn. 6.4}$$

where $A(0)$ is the unsupported ^{210}Pb inventory of the entire core. $A(m)$ and $A(0)$ are both determined by numerical integration of the ^{210}Pb profile, this equation gives the sediment age t as a function of depth m . The age of sediments at depth m is then given by

$$t = \frac{1}{\lambda} \ln \frac{A(0)}{A(m)}. \quad \text{eqn. 6.5}$$

Using this model it may also be shown that the (variable) sedimentation rate is given by the formula

$$r = \lambda A/C. \quad \text{eqn. 6.6}$$

Accuracy in the dating by this model, especially in the first few levels above the equilibrium depth is crucially dependent on reliable estimates of the ^{210}Pb inventories. Under-estimation of $A(0)$ will cause the ^{210}Pb dates of these levels to be too old.

6.3 Sediment Core Radionuclide Chronology

Sediments were dated using a combination of ^{210}Pb dating models and stratigraphic dating methods.

6.3.1 Chrono-stratigraphic dates

In all three cores the ^{137}Cs and ^{241}Am concentration depth profiles (Figs. 5.6-5.8) contain well resolved peaks identifying the depths of sediments recording fallout from the 1986 Chernobyl accident and the 1963 fallout maximum from the atmospheric testing of nuclear weapons. The dates determined from these stratigraphic records are summarised in the following table.

Feature	BLT 96/A		BLT 96/D		BLT 96/J	
	Depth (cm)	±	Depth (cm)	±	Depth (cm)	±
1986 Chernobyl ^{137}Cs peak	6.25	1.75	8.5	1.5	15.5	2.5
1963 Weapons test fallout peak	19.5	1	18.5	2.5	32	2

Table 6.1: Radiocaesium chronology of Blelham Tarn sediment cores.

6.3.2 ^{210}Pb Dates

^{210}Pb dates were calculated using the CRS dating model (Appleby *et al.*, 1978). The results placed 1963 at a depth of 18.5 cm in BLT 96/A, 19.3 cm in BLT 96/D and 30 cm in BLT 96/J, in good agreement with the $^{137}\text{Cs}/^{241}\text{Am}$ results. The 1986 depths were 7.25 cm in BLT 96/A, 7.5 cm in BLT 96/D and 12.5 cm in BLT 96/J. Dates calculated using the CIC model were more irregular and agreed less with the $^{137}\text{Cs}/^{241}\text{Am}$ results. Corrections to the CRS model dates to reduce the small

discrepancies with the $^{137}\text{Cs}/^{241}\text{Am}$ dates were calculated using the methods and procedures described in Appleby and Oldfield (1983) and Appleby (1998). The results are shown in Fig. 6.2-6.4 and given in detail in Table 6.2-6.4.

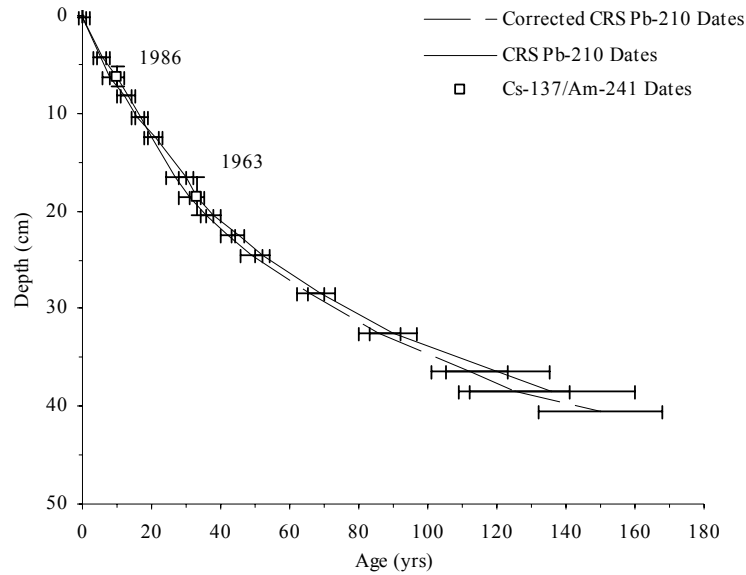


Fig. 6.2: CRS model ^{210}Pb dates in Blelham Tarn cores BLT 96/A. Also shown are the chronostratigraphic dates determined from the $^{137}\text{Cs}/^{241}\text{Am}$ stratigraphy, and the corrected ^{210}Pb dates.

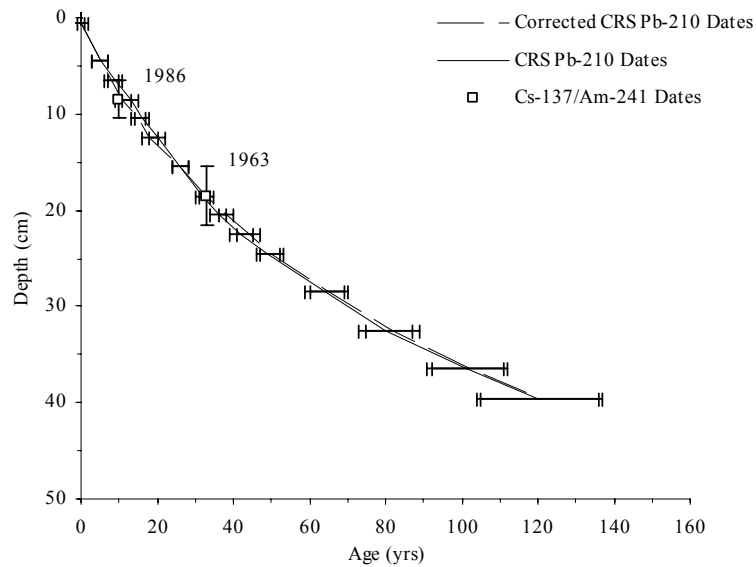


Fig. 6.3: CRS model ^{210}Pb dates in Blelham Tarn cores BLT 96/D. Also shown are the chronostratigraphic dates determined from the $^{137}\text{Cs}/^{241}\text{Am}$ stratigraphy, and the corrected ^{210}Pb dates.

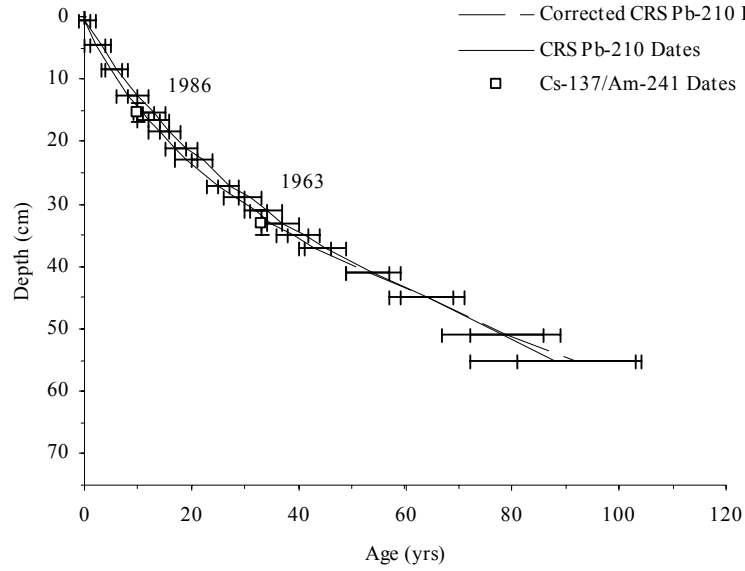


Fig. 6.4: CRS model ^{210}Pb dates in Blelham Tarn cores BLT 96/J. Also shown are the chronostratigraphic dates determined from the $^{137}\text{Cs}/^{241}\text{Am}$ stratigraphy, and the corrected ^{210}Pb dates.

Fig. 6.5 shows a comparison of sedimentation rates versus year in Blelham Tarn cores BLT 96/A, BLT 96/D and BLT 96/J and two further cores collected in 1997. All sites show significant increases in sedimentation rates after c. 1960. At sites B and J (near the head of the lake) there appears to have been a further significant acceleration in the 1980's. The very high sedimentation rates at site J presumably reflect the influence of catchment inputs via Ford Wood Beck and Hole House streams.

Depth		Chronology			Sedimentation Rate		
(cm)	(g cm ⁻²)	Date (AD)	Age (yrs)	±	(g cm ⁻² y ⁻¹)	(cm y ⁻¹)	± (%)
0.00	0.00	1996	0	0			
0.25	0.01	1996	0	1	0.064	0.63	5.9
4.25	0.42	1990	6	2	0.071	0.62	5.4
6.25	0.69	1986	10	2	0.086	0.53	6.2
8.25	1.03	1983	13	2	0.099	0.60	9.3
10.50	1.39	1979	17	2	0.101	0.63	11.3
12.50	1.74	1976	20	2	0.083	0.47	11.5
16.50	2.35	1969	27	3	0.086	0.61	17.3
18.50	2.63	1965	31	3	0.078	0.59	17.5
20.50	2.92	1961	36	2	0.055	0.35	10.2
22.50	3.22	1955	42	2	0.046	0.30	12.5
24.50	3.53	1948	49	3	0.040	0.24	12.0
28.50	4.21	1931	66	4	0.042	0.24	13.6
32.50	4.98	1911	86	6	0.034	0.17	20.3
36.50	5.81	1885	112	11	0.031	0.15	40.9
38.50	6.22	1872	125	16	0.027	0.14	68.9
40.50	6.67	1847	150	18	0.014	0.05	80.6

Table 6.2: Chronology of Blelham Tarn sediment core BLT 96/A.

Depth		Chronology			Sedimentation Rate		
(cm)	(g cm ⁻²)	Date (AD)	Age (yrs)	±	(g cm ⁻² y ⁻¹)	(cm y ⁻¹)	± (%)
0.0	0.00	1996	0	0			
0.5	0.02	1996	0	1	0.079	0.76	5.7
4.5	0.43	1991	5	2	0.086	0.74	6.7
6.5	0.70	1989	8	2	0.097	0.67	7.5
8.5	1.01	1985	11	2	0.082	0.55	8.1
10.5	1.30	1981	15	2	0.081	0.56	8.4
12.5	1.60	1978	18	2	0.069	0.51	8.7
15.5	2.01	1970	26	2	0.060	0.52	10.5
18.5	2.38	1963	33	2	0.054	0.47	11.1
20.5	2.62	1958	38	2	0.047	0.35	10.0
22.5	2.90	1952	44	3	0.051	0.35	13.5
24.5	3.22	1946	50	3	0.048	0.26	14.7
28.5	3.96	1931	65	5	0.051	0.27	22.7
32.5	4.81	1914	82	7	0.050	0.23	35.6
36.5	5.78	1894	102	10	0.044	0.16	43.2
39.5	6.60	1875	121	16	0.044	0.17	52.6

Table 6.3: Chronology of Blelham Tarn sediment core BLT 96/D.

Depth		Chronology			Sedimentation Rate		
(cm)	(g cm ⁻²)	Date (AD)	Age (yrs)	±	(g cm ⁻² y ⁻¹)	(cm y ⁻¹)	± (%)
0.0	0.00	1996	0	0			
0.5	0.06	1996	0	1	0.312	1.99	6.6
4.5	0.68	1994	2	2	0.293	1.67	7.3
8.5	1.42	1991	5	2	0.296	1.44	7.8
12.5	2.33	1988	8	2	0.300	1.42	8.4
15.5	3.05	1986	11	2	0.276	1.33	7.5
16.5	3.29	1985	12	2	0.212	0.88	7.8
18.5	3.75	1982	14	2	0.191	0.82	7.5
21.0	4.30	1979	17	2	0.180	0.81	6.9
23.0	4.75	1977	19	2	0.174	0.83	8.4
27.0	5.61	1971	25	2	0.124	0.56	7.2
29.0	6.02	1968	28	2	0.124	0.66	8.4
31.0	6.41	1964	32	2	0.112	0.57	8.4
33.0	6.80	1961	35	2	0.102	0.51	8.9
35.0	7.17	1957	39	3	0.100	0.58	10.3
37.0	7.54	1953	43	3	0.081	0.40	10.0
41.0	8.34	1943	53	4	0.077	0.37	13.2
45.0	9.18	1932	64	5	0.086	0.38	18.1
51.0	10.58	1917	79	7	0.092	0.41	29.6
55.0	11.60	1904	92	11	0.072	0.26	36.1

Table 6.4: Chronology of Blelham Tarn sediment core BLT 96/J.

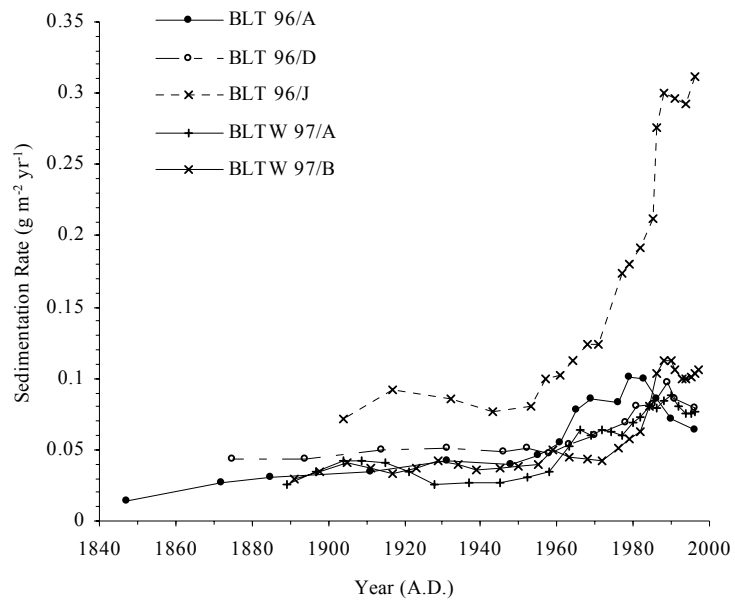


Fig. 6.5: Sedimentation rates versus year in Blelham Tarn cores BLT 96/A, BLT 96/D and BLT 96/J. Also shown are results from two further cores collected in 1997.

6.4 Peat Core Chronology

The chronology of the Foulshaw Moss peat core FLM 95 is given in Gedyes (1995). ^{210}Pb dates were calculated using the CRS model. Since peat deposits are subject to organic decay the CIC model is inappropriate to dating peat accumulations, even where there has been a constant growth rate (Appleby and Oldfield, 1992). The CRS model dates should however be unaffected by this process, provided there is no resultant displacement of the ^{210}Pb activity. The results, shown in Fig. 6.6 and Table 6.5, indicate a steady decline in net peat accumulation rates from *c.* $0.04 \text{ g cm}^{-2} \text{ yr}^{-1}$ in the upper sections of the core to *c.* $0.01 \text{ g cm}^{-2} \text{ yr}^{-1}$ below 16 cm. The ^{210}Pb dates put 1963 at a depth of 12 cm, in good agreement with the weapons test ^{137}Cs and ^{241}Am record.

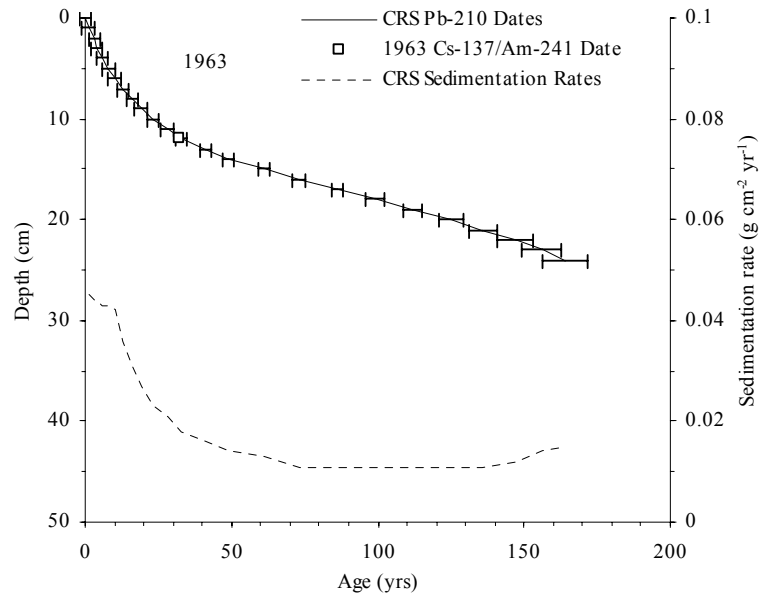


Fig. 6.6: CRS calculated age and sedimentation rate vs. depth plot for Foulshaw Moss peat core FLM 95 (Gedyes, 1995).

Depth		Chronology			Sedimentation Rate		
(cm)	(g cm ⁻²)	Date (AD)	Age (yrs)	±	(g cm ⁻² y ⁻¹)	(cm y ⁻¹)	±(%)
0.0	0.00	1995	0	2			
1.0	0.05	1994	1	2	0.045	0.70	5.5
2.0	0.12	1992	3	2	0.044	0.64	5
3.0	0.19	1991	4	2	0.044	0.57	4.3
4.0	0.27	1989	6	2	0.043	0.52	3.9
5.0	0.36	1987	8	2	0.043	0.48	4
6.0	0.45	1985	10	2	0.042	0.45	4
7.0	0.55	1982	13	2	0.036	0.38	4.1
8.0	0.65	1979	16	2	0.031	0.32	4.3
9.0	0.74	1976	19	2	0.027	0.28	5.2
10.0	0.84	1972	23	2	0.023	0.23	6
11.0	0.94	1967	28	2	0.021	0.19	5.2
12.0	1.04	1962	33	2	0.018	0.15	4.3
13.0	1.17	1954	41	2	0.016	0.13	4.6
14.0	1.30	1946	49	2	0.014	0.10	4.9
15.0	1.45	1934	61	2	0.013	0.09	6
16.0	1.60	1923	73	2	0.011	0.08	7.2
17.0	1.75	1910	86	2	0.011	0.08	8.2
18.0	1.89	1897	99	3	0.011	0.08	9.3
19.0	2.03	1884	112	3	0.011	0.08	11
20.0	2.17	1871	125	4	0.011	0.08	13
21.0	2.29	1860	136	5	0.011	0.09	18
22.0	2.41	1849	147	6	0.012	0.10	24
23.0	2.53	1840	156	7	0.014	0.12	31
24.0	2.64	1831	164	8	0.015	0.14	38

Table 6.5: Chronology of Foulshaw Moss core FLM 95 (Gedyes, 1995).

6.5 Sediment Core Trace Metal Chronology

The sediment chronology given in Table 6.2-6.4 can be used to calculate the rate of supply of trace metals to the sediment record through time. At a very simple level, if $r(t)$ denotes the sedimentation rate (in g cm⁻² y⁻¹) and $C(t)$ denotes the trace metal concentration (in μg g⁻¹) at time t , the flux to the sediments (in μg cm⁻² y⁻¹) at time t is

$$F(t) = r(t) \times C(t) \quad . \quad \text{eqn. 6.7}$$

In these calculations there are however a number of issues that need to be addressed. The total concentration C has two components:

- (i) background component C_{bg} deriving from the in-situ mineralogy of the soils and sediments, and

- (ii) an anthropogenic component C_{anth} deriving from atmospherically delivered pollution.

The anthropogenic component can itself be divided into two parts:

- (i) a component C_{dir} deriving from direct fallout onto the lake itself, and
- (ii) a component C_{cat} deriving from fallout onto the catchment stored in the soils and released slowly to the lake (via *e.g.* soil erosion).

The indirect component may include contributions from atmospheric pollution spanning hundreds of years.

A further issue is post-depositional redistribution within the sediment record by physical mixing of the surficial sediments during incorporation in the sediment record, or by advection and/or diffusion of a soluble component in the pore waters.

6.5.1 Background Values

In all of the sediment cores collected in 1996 the true trace metal background for these cores was not reached. In particular, the lead background of BLT 96/A was almost definitely not reached since sediment cores collected from the same location in 1997 (Appleby *et al.*, 1999) with longer records dating back several hundred years appear to reach background lead *c.* 40-50 mg kg^{-1} . Results from a Swiss peat bog (Shotyk *et al.*, 1998) indicate that atmospheric lead fluxes during mediaeval times were *c.* 0.05 $\mu\text{g cm}^{-2}\text{y}^{-1}$. Since the sedimentation rates in Blelham Tarn prior to *c.* 1800 were *c.* 0.025-0.05 $\text{g cm}^{-2}\text{y}^{-1}$, the direct fallout contribution to total lead concentrations during mediaeval times will have been just *c.* 1-2 mg kg^{-1} . These background concentrations can thus be regarded as a good estimate of the minerogenic component. Concentrations considered to represent background values are summarised in Table 6.6. These are from the two wide-diameter cores and several bulk cores collected as part of the European Transuranics programme (Appleby *et al.*, 1999).

Variations in trace metal background values within the Blelham basin are very apparent. Cu has the most stable background around 20 mg kg^{-1} , Pb and Zn show the most variation with values between 35 and 140 mg kg^{-1} 102 and 265 respectively.

Core	Depth	Depth	Pb	Zn	Cu	Ni
	m	cm	mg kg^{-1}	mg kg^{-1}	mg kg^{-1}	mg kg^{-1}
BLTW 97/A	11	68.5	42.0	126	26.3	-
BLTW 97/B	13	91.0	45.0	136	18.1	-
BLT 97/21	5.5	88.5	28.3*	102	15.4	34.5
BLT 97/23	12	85.5	34.7	106	16.5	36.0
BLT 97/45	5.5	87	35.0	103	17.7	37.1
BLT 97/56	6	85.5	49.3	112	19.9	39.0
Means*			40.7	119	21.2	36.7

Table 6.6: Sediment core background concentrations. * Excluding the apparently anomalous BLT 97/21 value.

6.5.2 Trace Metal Fluxes

Fig. 6.7 plots the anthropogenic component of the trace metal flux to the sediments of Blelham Tarn versus time calculated using the formula

$$F_{anth}(t) = r(t) \times (C(t) - C_{bg}) \quad \text{eqn. 6.8}$$

where C_{bg} is the estimated background concentration. They include results from all three 1996 cores together with those from the two 1997 cores (Appleby *et al.*, 1999). Also shown are trace metal fluxes determined (using the same procedure) from Foulshaw Moss core FLM 95. The 1997 Ni results are not included since there does not seem to be a very clear atmospheric signal.

The Pb results are fairly consistent. High fluxes at BLT 96/J reflect focussing plus catchment inputs (the concentration profiles are all diluted near the top). The fluxes to Foulshaw Moss and Blelham Tarn are comparable. The peat bog suggests atmospheric deposition increases significantly after *c.* 1800 a period coinciding with the beginnings of the industrial revolution. The apparently higher flux to the sediments at this time may be due to inputs via the catchment.

The Zn flux determined from the peat bog is significantly lower than that of the tarn. The increase in the Zn flux also occurs much later (1850-1900) than that of Pb. Possible causes are: (i) Zn is more soluble, and therefore more mobile in peat, (ii) greater inputs to the lake following disturbances in the catchment (stream re-routing and lowering of the water level), (iii) Zn having a different source proportionation (*i.e.* between mining and smelting and fossil fuel combustion), or (iv) a combination of these factors.

The Cu flux from the peat bog is also lower than that of the tarn, and the flux increase is later (1850-1900) than that of lead and Zn. Due to known diagenetic factors affecting Cu core profiles (Hilton, *pers. comm.*) the sub-surface peak in the Cu profile of all cores should be disregarded.

In spite of the irregularities there is a fairly clear pattern. The sediment record indicates that trace metal fluxes have increased by an order of magnitude during the past 200 years. The contemporary Pb flux appears to be between 5-10 $\mu\text{g cm}^{-2} \text{y}^{-1}$ (leaving aside core J), the Zn flux 10-20 $\mu\text{g cm}^{-2} \text{y}^{-1}$, and the Cu flux 1-2 $\mu\text{g cm}^{-2} \text{y}^{-1}$.

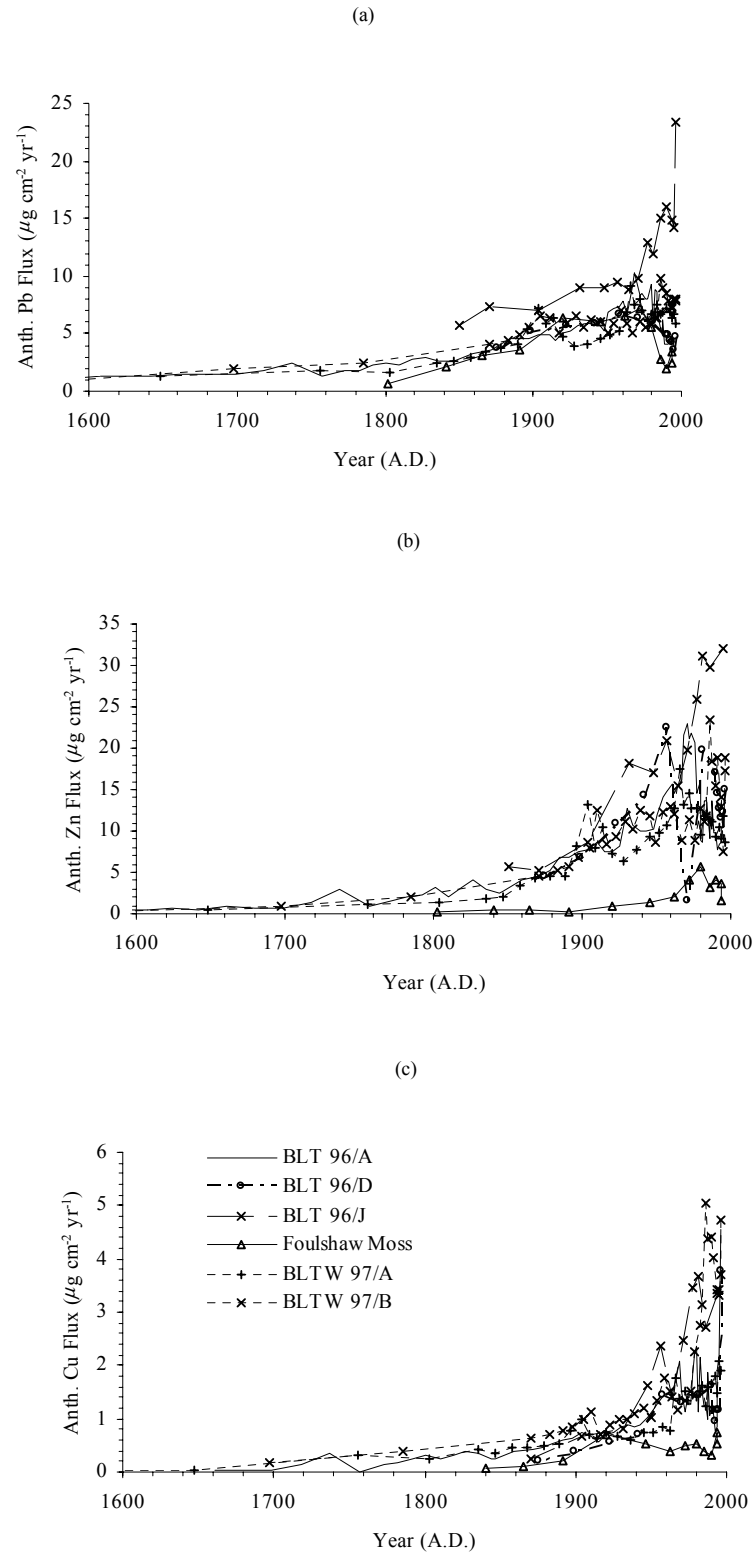


Fig. 6.7: Anthropogenic trace metal fluxes to the sediments of Blelham Tarn showing (a) Pb, (b) Zn and (c) Cu. Results from the 1996 cores are compared with those from two cores collected in 1997. Also shown are fluxes determined from the nearby Foulshaw Moss core FLM 95.